

NEAR-WALL MODELING OF LES FOR NON-EQUILIBRIUM TURBULENT FLOWS IN AN INCLINED IMPINGING JET WITH MODERATE RE-NUMBER

Y. LI¹, F. RIES¹, K. NISHAD¹ AND A. SADIKI^{1,2}

¹ Institute of Energy and Power Plant Technology
Technische Universität Darmstadt, 64287 Darmstadt, Germany
yongxiang.li@ekt.tu-darmstadt.de, www.ekt.tu-darmstadt.de

² Laboratoire de Genies des Procédés et Thermodynamique,
Institut Supérieur des Sciences et Techniques Appliquées,
Ndolo Kinshasa, RD Congo

Key words: LES, Near-Wall Modeling, Inclined Impinging Flow, Moderate Re-Number

Abstract. This paper reports on a comparative study of different near-wall modeling approaches in the context of large-eddy simulations (LES) under non-equilibrium flow conditions. For this purpose several LES with near-wall modeling of an inclined impinging jet at moderate Reynolds number of $Re = 5000$ are conducted and results are compared with near-wall flow statistics of a direct numerical simulation (DNS) dataset. Two commonly used wall stress models based on semi-logarithmic variation of the near-wall velocity, an advanced wall stress model that includes pressure gradient effects, a two layer approach and an improved delayed-detached eddy simulation method (IDDES) are evaluated. Thereby, it turned out that classical near-wall modeling treatments based on semi-logarithmic variation of the near-wall velocity do not apply under non-equilibrium flow conditions. In contrast, IDDES, two layer models as well as advanced wall function approaches that include pressure gradient effects are able to predict the near-wall flow statistics along with wall shear stresses properly. Furthermore, advanced wall function approaches exhibit significant lower computational cost compared to IDDES or two layer models. Because of this and due to their apparent simplicity, advanced wall functions might be a promising approach for near-wall modeling in real engineering applications.

1 INTRODUCTION

Impinging jets are used in a variety of engineering applications like cooling of gas turbine blades or electronic components because such flow arrangements provide a very effective and flexible way to transfer thermal energy between a target surface and a fluid. Given their practical relevance, several jet geometries and flow conditions were examined with the goal to identify preferred operating conditions along with guidelines for their

practical usage. Reviews of experiments, numerical studies and empirical correlations of impinging jet flows are provided by [1, 2] and others.

Characterized by strong flow/wall interaction processes, impinging flows feature very complex flow properties including the presence of stagnation point, shear boundary layer development, and strong streamline curvature [3], fundamentally different to those found in equilibrium boundary layer flows like turbulent pipe or channel flows. In the case of equilibrium boundary layers, the ratio of streamwise pressure gradient and wall shear stress is a constant and therefore a single velocity scale (i.e. the friction velocity) exists (see e.g. [4]). In contrast, in impinging flows an adverse non-streamwise pressure gradient force acts on the boundary layer and turbulence is predominantly imposed by the free stream and not wall shear generated as it is the case in equilibrium flows. Consequently, impinging boundary layers are highly non-equilibrium and no single velocity scale exists.

On the numerical modeling side, LES can provide insight into the complex flow dynamics of impinging flows. However, LES experiences severe shortcomings in dealing with near-wall dominated flows unless very fine grids are used in the vicinity of the wall. Thereby, in the so called wall-resolved LES approach, turbulent flow structures are fully resolved within the boundary layer resulting in very high computational cost. Therefore, due to limited computing power, it is common practice in LES to use a near-wall modeling approach to reduce the required computational effort, especially in the case of high Reynolds number flows where the boundary layer close to the wall becomes very thin. In general, these LES near-wall modeling approaches can be divided into wall shear stress, two layer and hybrid RANS/LES methods (see e.g. [5]).

Regarding wall shear stress models the very thin boundary layer at the wall is bridged with a single cell and suitable assumptions are made about the near-wall velocity profile in order to obtain the required wall shear stress. Because of bypassing the inner layer, the computational costs of this approach is noticeably lower than in wall-resolved LES and also lower compared to other near-wall modeling strategies like two layer models or hybrid RANS/LES. Classical wall function formulations are based on semi-logarithmic variation of the near-wall velocity like Spalding's wall function [6] or the approach proposed by Werner and Wengler [7]. However, it is well known that such simplified formulations do not apply under non-equilibrium flow conditions as apparent in impinging flows. To overcome this weakness, advanced wall treatments like generalized or analytical wall functions [8, 9] can be used that includes additionally pressure gradient effects.

In the case of two layer methods, a mesh with fine resolution is embedded between the matching location of the outer mesh and the wall. At the embedded mesh a simplified set of RANS-based turbulent boundary-layer equations are solved where the required wall shear stress is calculated and used as wall boundary condition for the LES calculation on the overlapped outer mesh. Pressure gradient effects are taken into account from the solution of the RANS-based turbulent boundary-layer equations. Therefore, as it is the case for advanced wall functions, two layer models are able to capture some non-equilibrium effects. However, as it was observed in many numerical studies (e.g. [10]), two-layer models tend to overpredict the skin friction, which is caused by the addition of the resolved turbulent stress. Moreover, it should be noted here, that the generation of

two separate numerical grids can be challenging in the case of complex geometries.

In the last approach, the so called hybrid RANS/LES modeling, RANS equations are numerically solved in the inner layer, while LES equations are solved away from the wall. Several strategies can be used to switch between one model and the other, such as changing the length scale from a RANS mixing length scale to a grid size related length scale, or using a blending function to merge the RANS and sub-grid scale eddy viscosities [5]. In contrast to wall-resolved LES, where the grid has to be refined isotropically in all three directions in the vicinity of the wall, hybrid RANS/LES requires only grid refinement in wall-normal direction, leading to a significant reduction in the computational cost [11]. Prominent examples of hybrid RANS/LES models are detached-eddy simulations (DES), very large-eddy simulations (VLES) or scale-adaptive simulations (SAS). Models of this type perform well in cases with mean-flow perturbations (adverse pressure gradients, separation), but can mismatch for flows with attached, thin shear layers, where the instability mechanisms are comparatively weak, as shown by [12].

Although numerous LES near-wall modeling approaches were proposed in the literature, it is worth mentioning that an assessment of the prediction accuracy and computational cost of these models regarding impinging flows among other complex flow situations are rarely reported in the literature. This motivates the present work, which reports on a comparative study of different near-wall modeling approaches in the context of LES under non-equilibrium flow conditions. For this purpose several LES with near-wall modeling of an inclined impinging jet at moderate Reynolds number of $Re = 5000$ are conducted and results are compared with near-wall flow statistics of a DNS dataset [3]. Two commonly used wall stress models based on semi-logarithmic variation of the near-wall velocity [6, 7], an advanced wall stress model that includes pressure gradient effects [8], a two layer approach based on the Spalart-Allmaras RANS model [13] and an improved delayed-detached eddy simulation method (IDDES) [14] are evaluated.

This paper is organized as follows. At first, the LES method and the near-wall modeling approaches are briefly described in section 2. Then, the numerical test case, an inclined impinging jet on a solid surface, and the numerical procedure are introduced in section 3. A validation of the near-wall modeling approaches under equilibrium flow conditions (fully developed turbulent channel flow at $Re_\tau = 2003$) is given in section 4. Subsequently, the results of the evaluation study for non-equilibrium fluid flow conditions are presented in section 5. Section 6 deals with a comparison of the computational cost of the different LES near-wall modeling approaches. Finally, some concluding remarks are provided in the last section.

2 METHODS

In this section, the LES and RANS equations applied to solve the turbulent flow field of the inclined impinging jet are introduced. Then, the near-wall modeling approaches used in the present study are briefly described.

2.1 LES and RANS equations

In the case of turbulent flow with constant physical properties and no body force the continuity and momentum equations with respect to RANS and LES read:

$$\frac{\partial \bar{U}_i}{\partial x_i} = 0 \quad (1)$$

$$\frac{\partial \bar{U}_i}{\partial t} + \frac{\partial}{\partial x_j} (\bar{U}_i \bar{U}_j) = -\frac{\partial \bar{p}}{\partial x_i} + \frac{\partial}{\partial x_j} \left((\nu + \nu_t) \left(\frac{\partial \bar{U}_i}{\partial x_j} + \frac{\partial \bar{U}_j}{\partial x_i} \right) \right), \quad (2)$$

where U_i is the velocity field, p the kinematic pressure, and ν the kinematic viscosity.

In the context of LES, $(\bar{\cdot})$ in equations 1 and 2 denotes filtered quantities, and ν_t represents the subgrid-scale eddy viscosity. Regarding RANS, $(\bar{\cdot})$ denotes time-averaged quantities, and ν_t is the turbulent eddy viscosity. In this work, the Wall-Adapting Local Eddy-Viscosity model (WALE model) [15] is selected to close the LES equations. Regarding RANS, the Spalart-Allmaras model [13] is used to close the RANS equations. The different near-wall modeling approaches to describe the boundary layer in the vicinity of the wall are described in the following.

2.2 Near-Wall Modeling: Wall Shear Stress Models

As mentioned above, the basic idea of wall shear stress models are to make suitable assumptions about the near-wall velocity profile in order to obtain the required wall shear stress τ_w . The most well-known assumption about the near-wall velocity profile is the law of the wall, which is based on equilibrium flow and reads:

$$U^+ = y^+ \quad (\text{near-wall region}) \quad U^+ = \frac{1}{\kappa} \ln y^+ + 5.2 \quad (\text{log law region}), \quad (3)$$

where $\kappa = 0.41$ is the Kármán constant. $U^+ = U/u_\tau$ and $y^+ = u_\tau y/\nu$ denote the velocity and the distance from the wall in wall units.

Based on the law of the wall, Spalding proposed a single formula for the whole boundary layer which includes viscous sublayer, buffer layer and inertia sublayer as [6]:

$$y^+ = U^+ + 0.1108 \left(\exp(\kappa U^+) - 1.0 - \kappa U^+ - \frac{(\kappa U^+)^2}{2!} - \frac{(\kappa U^+)^3}{3!} - \frac{(\kappa U^+)^4}{4!} \right), \quad (4)$$

whereby the wall stress can be obtained by a iterative procedure. A similar approach was proposed by Werner and Wengle [7], in which an analytical integration of a power-law near-wall velocity distribution resulting in the following expressions for the wall stress:

$$\tau_w = \begin{cases} \frac{2\nu|\bar{U}|}{\Delta y} & \text{for } |U| \leq \frac{\nu}{2\Delta y} A^{\frac{2}{1-B}} \\ \left[\frac{1-B}{2} A^{\frac{1+B}{1-B}} \left(\frac{\nu}{\Delta y} \right)^{1+B} + \frac{1+B}{A} \left(\frac{\nu}{\Delta y} \right)^B |U| \right]^{\frac{2}{1+B}} & \text{for } |U| > \frac{\nu}{2\Delta y} A^{\frac{2}{1-B}}, \end{cases} \quad (5)$$

where $A = 8.3$, $B = 1/7$ and Δy is the distance between the first cell center and the wall.

As it can be seen from equations 4 and 5, both, Spalding’s wall function and the approach of Werner and Wengle do not consider the effect of pressure gradients. To overcome this weakness, Shih et al. [8] proposed an extended formulation that includes the effects of the pressure gradient. Thereby, the velocity U is decomposed into two parts:

$$U = U_1 + U_2. \quad (6)$$

Here, U_1 depends only on the wall stress τ_w while U_2 is related to the streamwise pressure gradient dP_w/dz near the wall. Shih et al. proposed then the following formulations:

$$y_\tau^+ = U_1^+ + 0.1108 \left(\exp(\kappa U_1^+) - 1.0 - \kappa U_1^+ - \frac{(\kappa U_1^+)^2}{2!} - \frac{(\kappa U_1^+)^3}{3!} - \frac{(\kappa U_1^+)^4}{4!} \right), \quad (7)$$

$$(y_p^+)^2 = U_2^+ + 0.0408 \left[\exp(U_2^+/5.0) - 1.0 - U_2^+/5.0 \right], \quad (8)$$

where $U_1^+ = U_1/u_\tau$, $y_\tau^+ = y u_\tau/\nu$, $U_2^+ = 2U_2/u_p$ and $y_p^+ = y u_p/\nu$. u_p is calculated as $u_p = [(\nu/\rho)|dp_w/dz|]^{1/3}$ and u_τ is obtained by expression 7 using an iterative procedure. Using both velocity scales, the resulting velocity at the first grid point at the wall results from equation 6. A detailed description of the entire procedure can be found in [8].

2.3 Near-Wall Modeling: Two Layer Model

In the two layer approach, a mesh with fine resolution is embedded between the matching location of the outer mesh and the wall [17]. In the present study, the Spalart-Allmaras [13] model are applied to solve the inner layer on the embedded mesh which reads

$$\begin{aligned} \frac{\partial \tilde{\nu}}{\partial t} + u_j \frac{\partial \tilde{\nu}}{\partial x_j} &= c_{b1}(1 - f_{t2})\tilde{S}\tilde{\nu} - \left[c_{w1}f_w - \frac{c_{b1}}{\kappa^2}f_{t2} \right] \left(\frac{\tilde{\nu}}{d} \right)^2 \\ &+ \frac{1}{\sigma} \left[\frac{\partial}{\partial x_j} \left((\nu + \tilde{\nu}) \frac{\partial \tilde{\nu}}{\partial x_j} \right) + c_{b2} \frac{\partial \tilde{\nu}}{\partial x_i} \frac{\partial \tilde{\nu}}{\partial x_i} \right], \end{aligned} \quad (9)$$

where the turbulent eddy viscosity is calculated as $\nu_t = \tilde{\nu} f_{v1}$. The model coefficients employed in the present study can be found in [13]. On the outer layer, the LES equations are solved using the WALE model [15]. Thereby the resolved velocity and pressure gradient from the LES serve as boundary condition for the inner layer RANS. Finally, the wall stress from the RANS is returned as wall boundary condition for the LES calculation.

2.4 Near-Wall Modeling: Improved Delayed Detached-Eddy Simulation

Following the procedure described in [14], a hybrid turbulent length-scale based on the blending of the RANS and LES length-scales are used in the improved delayed detached-eddy simulation (IDDES) approach. The length scale is given as:

$$\tilde{l} = f_h(1 + f_{restore}\Psi)l_{RANS} + (1 - f_h)\Psi l_{DES}, \quad (10)$$

where l_{RANS} is a RANS-based turbulent length scale and l_{DES} is a grid-based length scale. In the case of Spalart-Allmaras model as applied in the present study, the RANS-based

length scale equals the distance to the wall $l_{RANS} = d_w$. The grid-based length scale is calculated as $l_{DES} = C_{DES}\Delta$, where Δ is the grid width defined as $\Delta = (\Delta_x\Delta_y\Delta_z)^{1/3}$ and C_{DES} is a constant given as $C_{DES} = 0.65$. In the IDDES approach, the blending function f_h is defined in such a way that l_{RANS} is used in regions with low mesh resolution (primarily close to the wall) and l_{DES} in region where the grid resolution is sufficient fine for LES (away from the wall). A detailed description of the model can be found in [14].

3 Configuration and numerical Procedure

In accordance with the DNS study [3], a turbulent jet impinging on a 45°-inclined solid surface at $Re = 5000$ is investigated. Figure 1 (A) shows a contour plot of the instantaneous magnitude velocity $|U|$ at mid-plane section of the jet. Notice that an additional coordinate system is introduced with η representing the wall-normal direction and ζ is the direction along the wall with the origin located at the stagnation point.

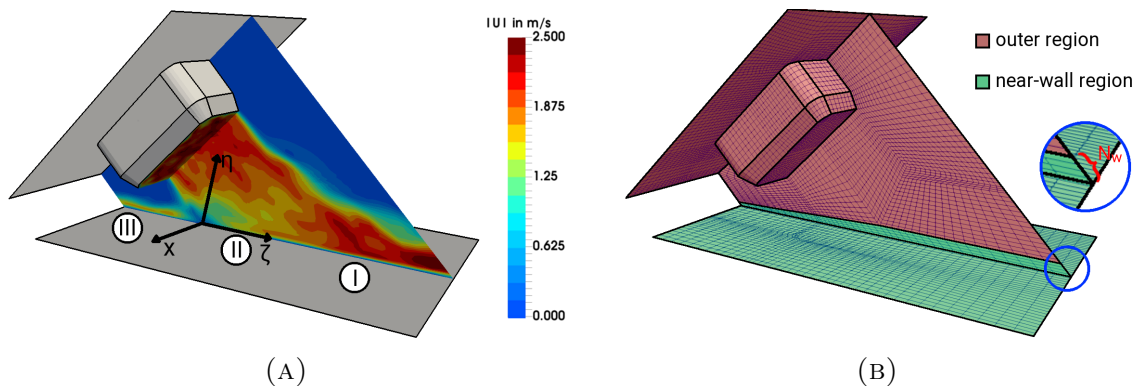


FIGURE 1. Snapshot of the magnitude velocity at mid-plane section (A) and a representation of the numerical grid (B) of the inclined impinging jet configuration.

In the test section, a turbulent stream of dry air ($T = 290K, p = 1atm, Re = 5000$) leaves a square nozzle (diameter $d = 40mm$) and is blocked after a distance of $1D$ by a 45°-inclined wall. Thereby, due to a turbulence generating grid located inside the nozzle (not shown here), the jet stream appears highly turbulent (turbulent intensity of 10%) and is not fully developed when it leaves the nozzle (see [3]). Further downstream, the main flow is divided into two opposed jet streams directed outward along the solid surface. As it can be seen in figure 1 (A), different flow situation associated with a characteristic near-wall behavior occur within this configuration, namely, (I) a wall-jet in main flow direction that resembles an equilibrium boundary layer, (II) a stagnation region with high non-streamwise pressure gradient force and (III) an opposed wall-jet region, where the fluid is subject to a strong acceleration, stretching and recirculation.

An illustration of the block-structured numerical grid used in the present study is shown in figure 1 (B). The grid is divided into an outer region and a near-wall region. The spatial resolution of the outer region is identical for all near-wall modeling approaches and consists of 86,677 control volumes. The resolution of the near-wall region depends on

the particular near-wall modeling approach applied. In this respect it is worth mentioning that a non-dimensional wall distance parameter to describe the near-wall resolution is not meaningful in the case of impinging flows since no single velocity scale exists. Therefore, for comparison reasons, the number of grid points in wall normal direction N_w within the near-wall region and the wall distance of the first grid cell at the wall η_w are used to characterize the near-wall resolution. Characteristic quantities of the numerical grids in respect to the particular near-wall modeling approaches are summarized in table 1.

TABLE 1. Spatial resolution of the numerical simulations. N : total number of cells; N_i : number of cells of the near wall region; N_w : number of cells in wall normal direction within the near-wall region; η_w : wall distance of the first grid cell at the wall.

	wall function	two layer	IDDES
N	90,941	103,733	99,469
N_i	4,264	12792	12792
N_w	2	6	6
η_w	0.50-1.25mm	0.11-0.28mm	0.11-0.28mm

Regarding the inlet condition at the nozzle exit section, realistic inflow data from the DNS study [3] are utilized. Therefore, the turbulent velocity field is recorded in the DNS at the nozzle exit section and stored for each time step in a database. These dataset is interpolated in space and time to match the inlet of the LES simulation. At the outflows, a velocity inlet/outlet condition is used to allow backflow into the computational domain. Thereby, the internal cell value is used in the case of inflow and Neumann condition is applied in the case of outflow. At the walls, no-slip condition is utilized.

LES with near-wall modeling is performed using the standard solver pimpleFoam of the open source C++ library OpenFOAM 2.4.0. The considered near-wall modeling approaches are added to the source code. A second order central differencing scheme is applied for the convection terms and a second order conservative scheme is used to solve the Laplacian terms. A second order backward integration method is utilized for the time derivative terms. Thereby, the time step is chosen small enough to ensure that the CFL-number remains smaller than one. Convergence of the iterative procedure is obtained if all normalized residuals are smaller than 10^{-8} .

4 PREDICTION ACCURACY: EQUILIBRIUM CONDITIONS

At first the prediction accuracy of the models under equilibrium flow conditions is examined. For this purpose, LES with near-wall modeling of a fully developed channel flow at $Re_\tau = 2003$ is conducted and results are compared with a DNS of [18]. The dimensions of the domain are given as $10\delta \times 2\delta \times 25\delta$ in spanwise, wall-normal and streamwise direction, respectively, where δ is half the channel height. In the case of wall shear stress models the spatial resolution is selected as $(\Delta x^+, y_w^+, \Delta z^+) = (200, 80, 200)$

resulting in 1,250,000 cells. Regarding the two layer modeling approach the resolution of the outer mesh equals the numerical grid used for the wall shear stress models. The embedded mesh is located at $y^+ = 720$ and consists of 725,00 cells. For the IDDES, the mesh resolution is chosen as $(\Delta x^+, y_w^+, \Delta z^+) = (200, 1, 200)$ with a total number of cells of 2,375,000. Results of the predicted mean and rms velocities along the wall-normal direction in comparison with the DNS data are shown in figure 2.

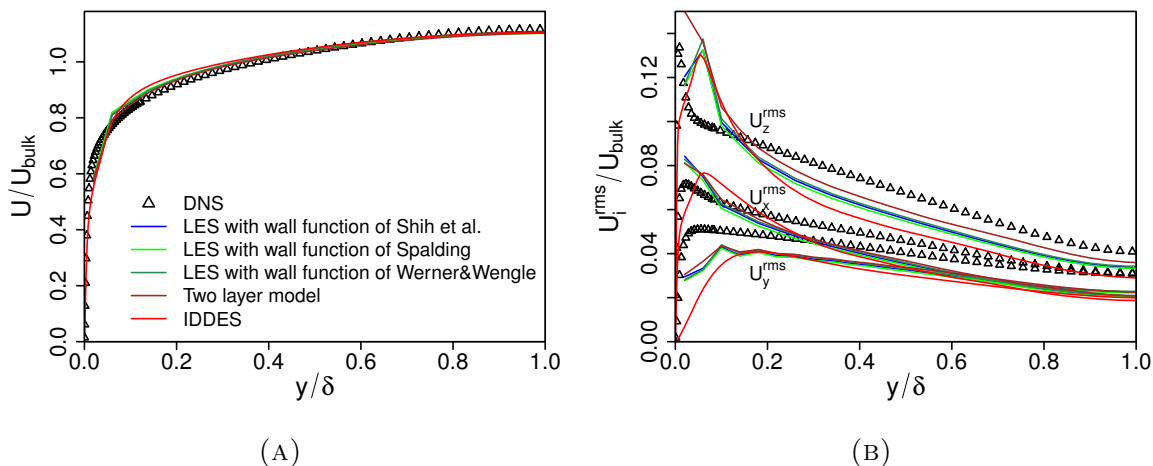


FIGURE 2. Profiles of predicted mean and rms velocities along the wall-normal direction using different LES near-wall modeling approaches. Comparison with DNS data of [18].

As it can be seen in figure 2 (A) predicted mean velocities are in good agreement for all LES near-wall modeling approaches. Similar results are obtained for the rms velocity profiles. However, the peak values of the rms velocities are slightly shifted away from the wall and values at the outer region are underestimated, which holds for all models.

Finally, predicted wall shear stresses of the different near-wall modeling approaches are compared with the DNS value in table 2.

TABLE 2. Predicted wall shear stresses in comparison with the DNS value.

	Shih	Spalding	Werner&Wengler	two layer	IDDES
τ_w/τ_w^{DNS}	0.91	0.86	0.91	1.03	0.73

Obviously, the wall shear stress is slightly overestimated by the two layer model and underestimated by the wall function and IDDES approaches. Best agreement is given by the two layer model, while the IDDES method reveals largest discrepancies.

5 PREDICTION ACCURACY: NON-EQUILIBRIUM CONDITIONS

After examining the performance of the LES near-wall models for equilibrium conditions, their prediction accuracy under non-equilibrium conditions is analyzed now. For

this purpose, figure 3 shows predicted wall-parallel (A) and wall-normal (B) mean velocities at several wall-normal traverses ($\zeta/D = -0.5, 0, 0.25, 0.5, 1$) of the inclined impinged wall in comparison with the DNS dataset of [3]. The corresponding rms wall-parallel and wall-normal velocity components are depicted in figure 3 (C) and (D), respectively.

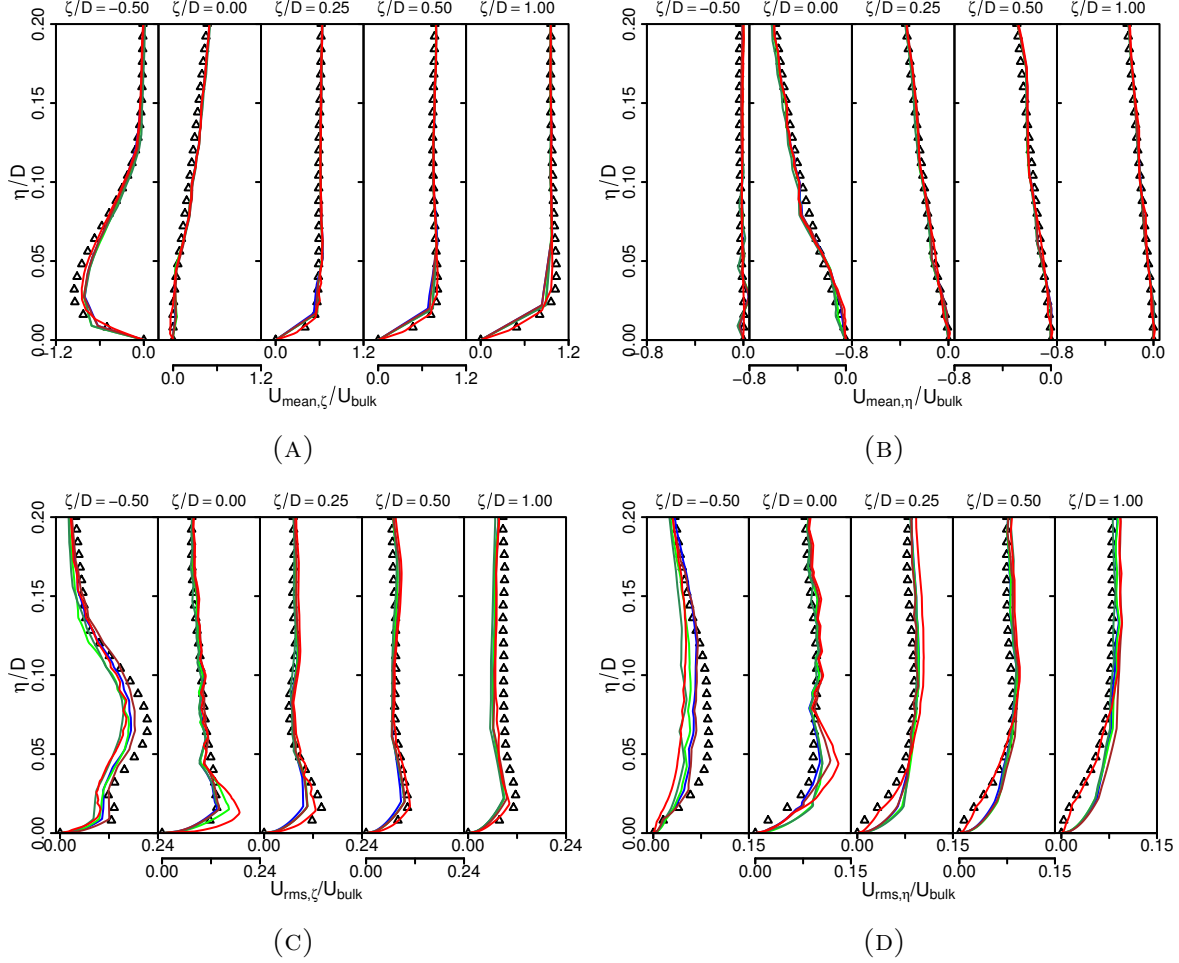


FIGURE 3. Time-averaged and rms wall-parallel (A), (C) and wall-normal (B), (D) velocity components divided by the bulk velocity of the jet at several wall-normal traverses (legend see figure 2).

Just as under equilibrium conditions, predicted mean velocity profiles agree very well with the DNS data. This holds for all LES near-wall modeling approaches under consideration. A similar conclusion can be drawn for the wall-parallel and wall-normal rms velocity profiles as shown in figure 3 (C) and (D), respectively. Here, deviations between the different LES near-wall modeling approaches are slightly higher, however all the models give reasonable results.

Figure 4 shows the predicted wall shear stresses along the wall-parallel direction ζ at $x/D = 0$ (at the stagnation region of the jet) in comparison to the DNS data of [3].

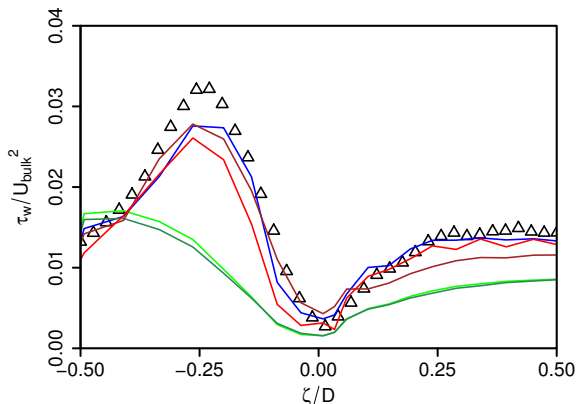


FIGURE 4. Predicted wall shear stress along the wall-parallel direction ζ at $x/D = 0$ in comparison to the DNS data of [3]. (legend see figure 2)

As it can be clearly seen in figure 4, the classical wall function formulations based on a semi-logarithmic variation of the near-wall velocity (Spalding [6] and Werner&Wengle [7]) underestimate the wall shear stress considerably and as a result do not apply under non-equilibrium conditions with strong non-streamwise pressure gradients. In contrast to these, the advanced wall function by Shih et al. [8], the IDDES method [14] and the two layer model do not show such a unphysical behavior. All these models are able to predict the wall shear stress around the stagnation point properly (as well as apart from it) and might be therefore a promising approach for near-wall modeling under such flow conditions.

6 COMPUTATIONAL COST

One of the key objectives by using near-wall modeling is to reduce the computational effort of a LES to allow the calculation of high Reynolds number flows. Therefore, it is of practical interest to address the required computational cost to achieve an acceptable prediction accuracy. For this purpose figure 5 shows the required relative computational cost of the different LES near-wall modeling approaches for the turbulent channel test case (A) and the inclined impinging jet configuration (B) with regard to the computational cost required by using Spalding’s wall function. The computational cost is estimated on a Linux 3.10.0-514.26.1.el7.x86_64 Red Hat 4.8.5-11 (x86_64) system using an Intel(R) Xeon(R) CPU X5660 with 2.80GHz and 48GiB RAM. 6 CPU-cores were used and the maximal CFL-number was set to 0.3.

Regarding the channel flow test case at high Reynolds number (figure 5 (A)), the computational cost is low for wall shear stress models and up to four times higher for the IDDES and two layer approaches. This picture changes in the case of the inclined impinging jet configuration. Here, all LES near-wall modeling approaches exhibit a similar computational cost due to the moderate Reynolds number. Therefore, it can be concluded that especially for high Reynolds number flows, wall shear stress models are less computational expensive than other LES near-wall modeling approaches, while in the case of

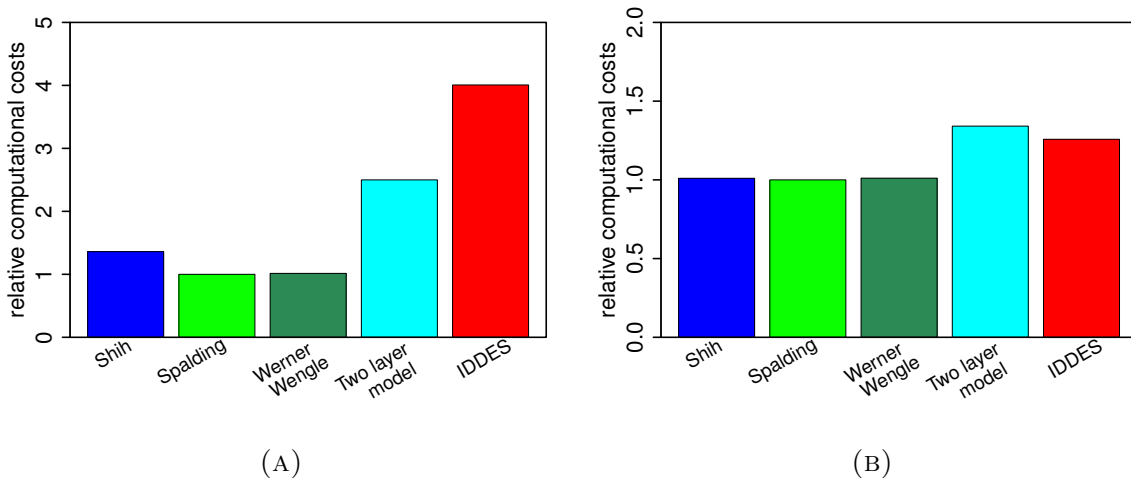


FIGURE 5. Relative computational cost of different LES near-wall modeling approaches for the turbulent channel test case (A) and the inclined impinging jet configuration (B) with regard to the computational cost required by using Spalding’s wall function.

moderate Reynolds numbers all models are similar CPU-intensive.

7 CONCLUSIONS

Several LES near-wall modeling approaches have been evaluated for equilibrium and non-equilibrium boundary layers. For this purpose LES with near-wall modeling have been conducted for a fully developed turbulent channel flow at a high Reynolds number of $Re_\tau = 2003$ and a turbulent jet impinging on a 45° -inclined solid surface at a moderate Reynolds number of $Re = 5000$. Thereby, the prediction accuracy and the relative computational cost of the different approaches have been determined. Some important observations from this comparative study can be outlined as follows:

- Examining turbulent near-wall flow statistics, it turned out that wall shear stress, IDDES and two layer models are able to predict mean and rms velocities appropriate for both equilibrium and non-equilibrium boundary layers.
- Regarding wall shear stresses, advanced wall function approaches like the formulation of Shih et al. [8], IDDES and two layer models are able to predict the wall shear stress accurately for equilibrium and non-equilibrium boundary layers.
- Regarding the computational cost of different LES near-wall approaches, it appears that especially for high Reynolds number flows, wall function models are less computational expensive than IDDES or two layer models, while in the case of moderate Reynolds number flows all these models are similarly CPU-intensive.

REFERENCES

- [1] Zuckerman, N. and Lior, N. Jet Impingement Heat Transfer: Physics, Correlations, and Numerical Modeling. *Adv Heat Transfer* **2006**, *39*, 565–631

- [2] Martin, H. Heat and mass transfer between impinging gas jets and solid surfaces. *Adv Heat Transfer* **1997**, *13*, 1–60
- [3] Ries, F. et al. Database of near-wall turbulent flow properties of a jet impinging on a solid surface under different inclination angles. *Fluids* **2018**, *3(1)*, 5
- [4] Clauser, F. H. Turbulent Boundary Layers in Adverse Pressure Gradients. *J Aeronaut Sci* **1954**, *21*, 91–108
- [5] Piomelli U. Wall-layer models for large-eddy simulations. *Prog Aerosp Sci* **2008**, *44*, 437–446
- [6] Spalding DB. A Single Formula for the Law of the Wall. *ASME. J. Appl. Mech* **1961**, *28*, 455–458
- [7] Werner H. and Wengle H. Large-Eddy Simulation of Turbulent Flow Over and Around a Cube in a Plate Channel. *Turbulent Shear Flows 8* **1993**. 155–168
- [8] Shih, T.-H. et al. A generalized wall function, NASA Report No. TM-1999-209398, **1999**.
- [9] Craft, T. J. et al. Progress in the generalization of wall-function treatments. *Int J Heat Fluid Fl* **2002**, *23*, 148-160
- [10] Balaras, E. et al. Two-layer approximate boundary conditions for large-eddy simulations. *AIAA J* **1996**, *34*, 1111–1119
- [11] Hasse C. Scale-resolving simulations in engine combustion process design based on a systematic approach for model development. *Int J Engine Res* **2016**, *17*, 44–62
- [12] Shih, T.-H. et al. Application of generalized wall function for complex turbulent flows. *J Turbul* **2003**, *4*, 015
- [13] Spalart, P. and Allmaras, S. A one-equation turbulence model for aerodynamic flows, *30th aerospace sciences meeting and exhibit*, **1992**.
- [14] Travin A.K. et al. Improvement of delayed detached-eddy simulation for LES with wall modelling. *European conference on computational fluid dynamics ECCOMAS CFD 2006*, TU Delft, **2006**. pp. 41032.
- [15] Ducros, F. et al. Wall-adapting local eddy-viscosity models for simulations in complex geometries. *Numer. Methods Fluid Dyn. VI*, **1998**.
- [16] Pope. S. B. *Turbulent flows*, IOP Publishing, **2001**. ISBN 978-0-521-59886-6.
- [17] Balaras, E. and Benocci C. Subgrid-scale models in finite-difference simulations of complex wall bounded flows. In: AGARD CP 551, Neuilly-sur-Seine, France, **1994**.
- [18] Hoyas, S. and Jiménez, J. Scaling of the velocity fluctuations in turbulent channels up to $Re_\tau = 2003$. *Phys. Fluids* **2006**, *18*, 011702